Chapter – 5

PALEOSTRESS PATTERN

The morphotectonic domain-I is occupied by southward flowing three major river basins vis., Dhantarvadi, Raidi and Malan (from east to west). It is structurally controlled terrain mainly comprising NE-SW to NNE-SSW trending dyke ridges, NW facing vertical escarpments in cuesta ridges, coastward tilted trappean lava flows and fault offsetting ridges. Towards south, very gently coastward dipping Tertiary rocks overlying the pediment surface shows two prominent joint sets. The lava flows and fossiliferous limestone shows gentle coastward dip. The thin coastal strip occupying Quaternary deposits mainly miliolites, sandy beaches and intertidal flats. The coastal geomorphic features observed are alternate beach dune complexes and ~5 to ~25 m high marine cliffs with notches, sea caves, sea arcs and extensive mudflats. The domain shows structural lineaments with NE-SW as prominent trend due to dyke ridges. For the present study, structural attributes like faults and joints are investigated to understand the overall tectonic set up and stress pattern.

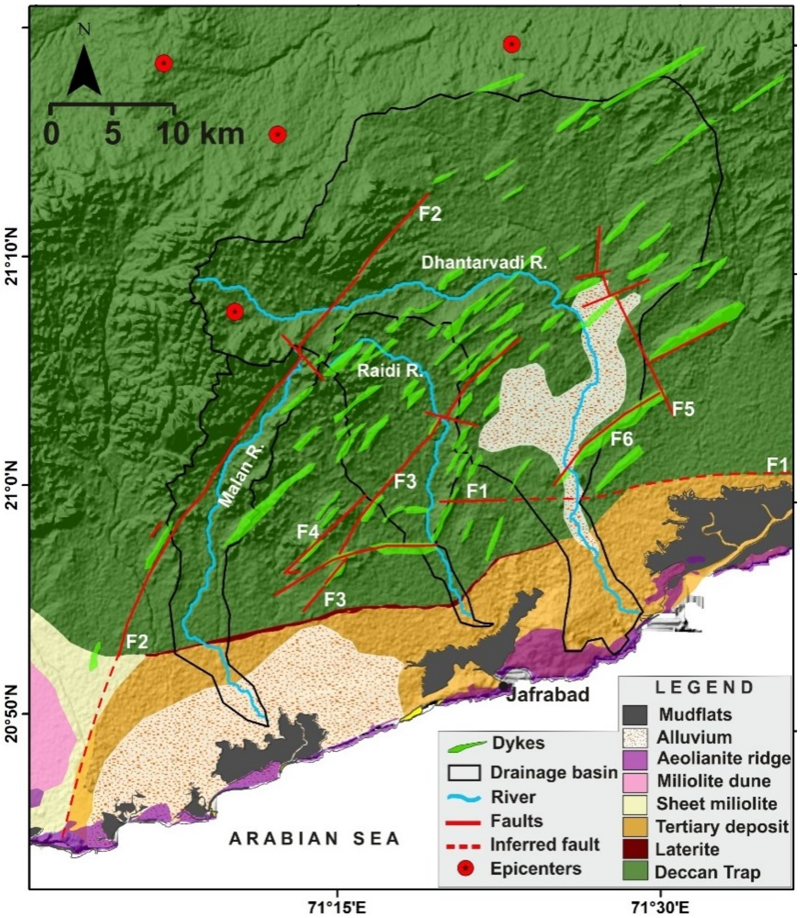

Figure 5.1 Geological map of morphotectonic domain-I superimposed over DEM. Note the dyke ridges that correspond to the swing of dyke swarm in Deccan traps.

Faults (F1 to F6) mapped during the present study, dyke ridges and drainage basins. Red circles showing earthquake epicenters.

5.1 MAJOR FAULTS

Several faults are mapped in the trappean basaltic region covering most of the entire upland area over Deccan traps. The remote sensing studies and detailed field investigation lead to several faults which are previously unreported. There is no information available on the tectonic and structural setting of these faults. Hence, it was found necessary to map all the faults investigated and to understand its impact on the landscape of this domain.

5.1.1 Katar Fault (F1)

Katar Fault is over a ~ E trending ~ 1 km long ridge W to the Katar village near the Rajula town, South Saurashtra. The Katar ridge was first selected using the Google Earth image along with the Survey of India topographical maps. The fault has been identified as east trending almost vertical fault planes (Figure 5.2) based either on prominent striation-bearing fault planes, or by noting P-planes almost perpendicular to those fault planes, i.e., on ~ horizontal planes. There are three categories of striations noted: horizontal, vertical and oblique (Figure 5.3a-d). At few places, P- and Y- brittle shear planes were observed where the sigmoid P-planes merge ~ tangentially with the Y-planes indicating sinistral (Figure 5.3e-g).

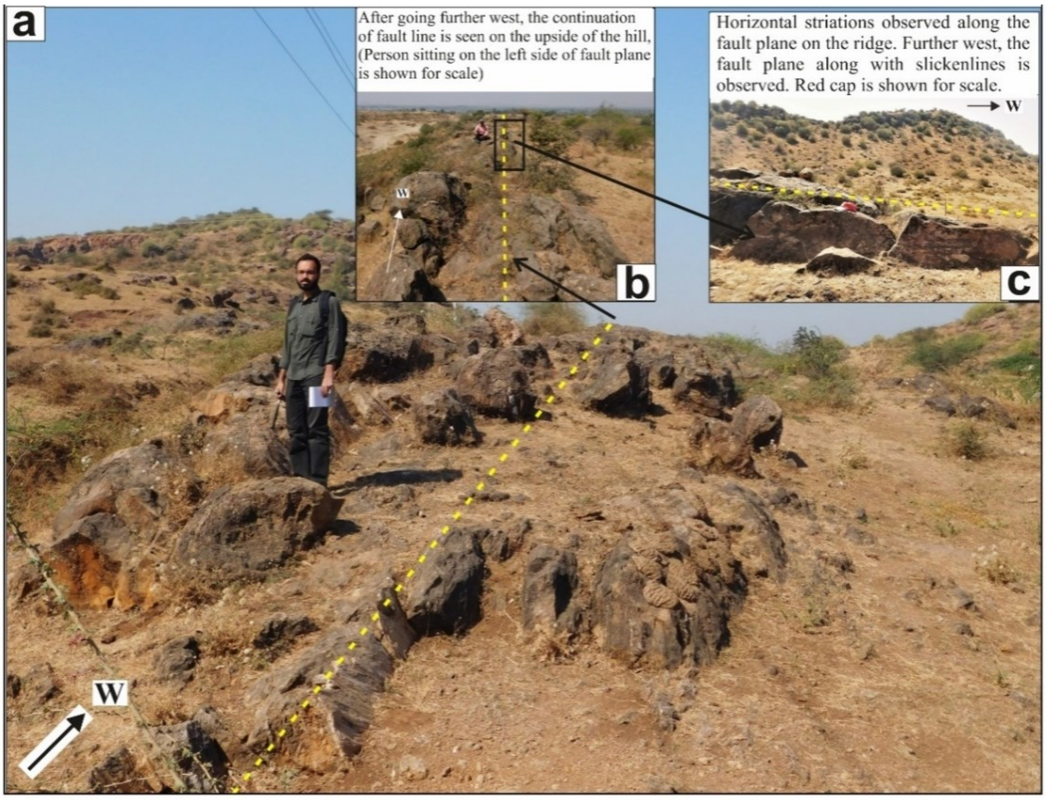

Figure 5.2 The E-W trending Katar fault exposed west of Rajula town. (a) Meso-scale fault cuts the Katar Ridge. Yellow dotted line: fault plane. Height of the person is 175

cm as scale. The fault line continues further towards W, as in photo. (b) These fault planes show different types of striations: such as horizontal in photo. (c) Red cap as scale. The fault cutting the NW trending ridge shows such slickensides.

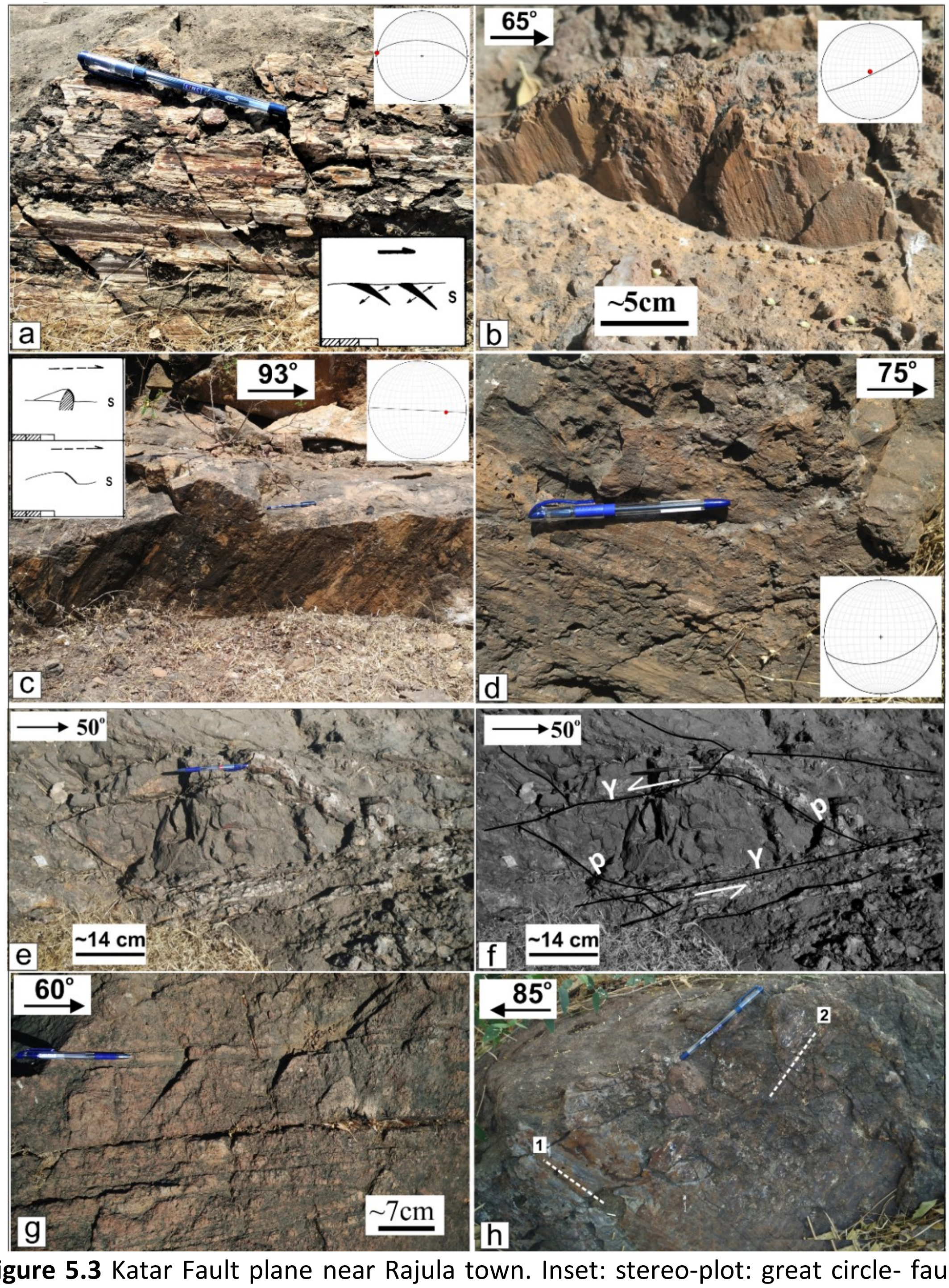

Figure 5.3 Katar Fault plane near Rajula town. Inset: stereo-plot: great circle- fault, red dot- lineation (Vanik et al., 2018). (a) Sub-vertical undulating fault plane (attitude: 93° strike, 62° dip, 3° dip direction) with horizontal striations. 14.3 cm long pen as scale. Fractures at high-angle to the fault. Inset: Fig. 1(FR) of Doblas et al. (1997). (b) Fault plane (attitude: 65° strike, 84° dip, 155° dip direction) with (sub) vertical striations. Damaged border and arrow-shaped micro-gouges define striation. Inset: Fig. 1 of Doblas et al. (1997). (c) Ridges and groove connoting oblique striations (rake 51°, trend 94°) on a fault plane (attitude: 93° strike, 90° dip, 3° dip direction). Slip sense indeterminate. 14.3 cm long pen as scale. (d) Very faint/poorly developed

(sub)horizontal lineations on sub-vertical fault plane (attitude: 75° strike, 54° dip and 165° dip direction). Inset: stereo-plot of faults with ENE trend. 14.3 cm long blue pen as scale. Un-interpreted (e) Interpreted (f) photograph: P- and Y- brittle shear planes trend NE on a horizontal plane on a basaltic rock. The sigmoid P-plane merging the Y-plane show sinistral slip. (g) P- and Y- brittle shear planes on a horizontal basaltic rock surface showing dextral slip. (h) A curvi-planar fault plane with two trends of oblique striations. A 14.3 cm long blue pen as scale. At "1", fault plane attitude: 285° strike, 70° dip, 15° dip direction. Striation plunge: 53°, trend: 315°. At "2", fault plane attitude: 109° strike, 73° dip, 19° dip direction. Striation with plunge: 35°, trend: 95°. Note the overlapping of oblique striations at the bottom of the field photograph.

P- and Y- brittle shear planes are considered reliable slip sense indicators (e.g., Means, 1987; Mukherjee and Koyi, 2010; Mukherjee, 2013, 2014, 2015a, b; Misra et al., 2014; Dasgupta and Mukherjee, 2017; Misra and Mukherjee, 2017).Slickenside striations with kinematic indicators like fractures perpendicular to the fault surface in the direction of movement have been observed on the megascopic-scale to identify the slip sense (Figure 5.3a-d). Sigmoid tension gashes, hybrid fractures and step-like indicators as slickolite markers (Doblas, 1998) were observed on the fault planes (Figure 5.3a, c). Most of the horizontal slickenside striations indicate dextral slip. There are few other (sub) horizontal striations with shear sense indicators which are also observed. Which faulted block exactly moved up or down was difficult to decipher from most of the vertical striations since they are indistinct kinematic indicators. However, features related to contraction like broken edges and arrow-shaped micro-gouges on the fault plane are identified as reliable kinematic indicators (Figure 5.3).

The steps or peaks face upslope indicating the slip sense (Figure 5.3c). Asymmetric curved elevations, peaks and step like features on the rock surface have been observed in oblique striated planes. Depending on the friction between the slipping fault blocks, the orientation of steps rises towards the motion of the opposite block. In few cases the slip sense was deciphered by moving hand softly parallel to the slickensides to know the positive and negative smoothness criterion i.e., finding out the direction of smoothness (Doblas, 1997; 1998).Oblique striations mostly indicate reverse faulting (Figure 5.3c). The sense of shear at these sub-vertical fault planes appears to be either horizontal (i.e. strike-slip) or oblique (i.e., oblique-slip). In one of the sub-vertical fault planes, two different trends of oblique striations have also been observed (Figure 5.3h).

5.1.2 Fault (F2)

This fault (F2) forms the western margin of the morphotectonic domain-I is a mega-lineament also considered as fault in the SW region crossing ~E-W flowing Dhantarvadi River in the north, continues along ~NE-SW flowing Malan River and then crosses ~NW-SE flowing Rawal River near Mota Samadhiyala village (Figure 4.1). The fault also further extends several kilometers towards SSW which is detected in the remote sensing data and Google Earth Pro. This was detected due to the topographical variation in the same trappean lithology of Deccan Trap formation on either side (Figure 4.4a-b). The field details of the fault exposed at accessible areas were mapped.

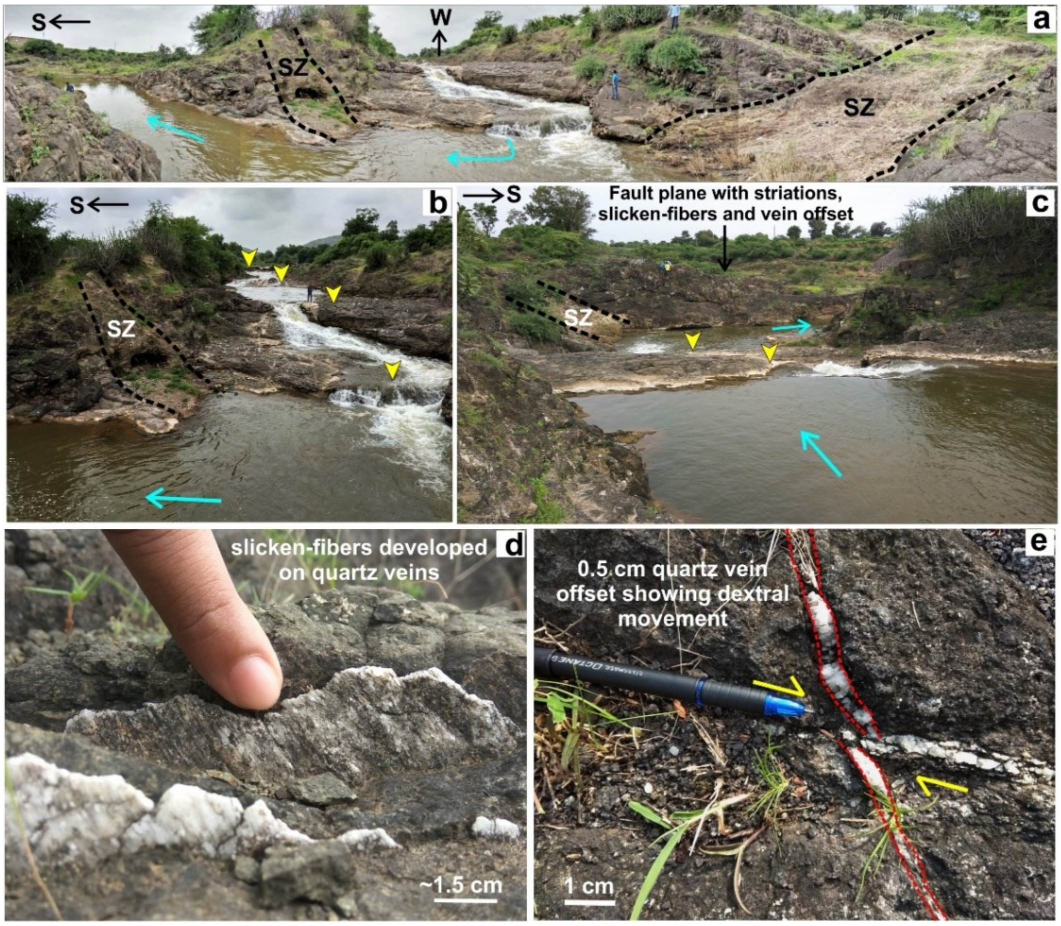

Figure 5.4 NE-SW trending fault exposed in E flowing Dhantarvadi River, west of Khambha village. a) River meandering near NNE trending shear zone (SZ). Note the knickpoints in the upstream direction d) Yellow arrow shows four knickpoints at every few meters. Note the gradient change from the farthest knickpoint up to shear zone. e) Opposite view of (d) showing fault plane with striations, slicken-fibers on quartz veins. Yellow arrow shows knickpoints. f) Close view of slicken-fibers developed on quartz veins showing oblique striations. g) 0.5 cm quartz vein offset on the fault plane within the joints showing dextral movement.

To the west of Khambha village, on the eastward flowing Dhantarvadi River, at the confluence of the main trunk stream and a small tributary, there is ~NE-SW trending shear zone/fault plane observed crossing the River (Figure 5.4b, c). The lithology comprises of highly jointed and fractured basaltic ridge where river is incising the weak (sheared) zone with a sharp bend towards south and then flows eastward (Figure 5.4 b-e). There is a very strong vein activity observed all along this shear zone which got eroded by river. Towards the upstream, four knickpoints observed at every few meters (Figure 5.4d). The ~1 m knickpoint observed close to the fault pane and towards upstream ~2m, ~1m and the farthest one was ~1m high. The change in slope of the river bed from the fault plane to the last knickpoint (recent) is approx. 6 to 8m.The migration of knickpoints towards the upstream was clearly observed retreating the trappean ridge (Figure 5.4b-d). This resulted in the sharp gradient change from the last visible knickpoints up to the fault zone.

The elevation of the fault plane is ~206 m amsl and ~6-7m from the river bed (Figure 5.4e). The slicken-fibers was well developed on the quartz veins within the joints on the fault plane (Figure 5.4f). The vertical as well as oblique striations was also observed along with enormous amount of joints and fractures at several places on the fault plane. The sense of slip observed in the field inferred that the fault is normal dextral. Apart from this, on the horizontal surface on the fault plane, brittle shear zones were clearly seen with P- and Y- planes. These planes were indicating top to SW brittle shear. A few cm vein displacement was also observed near the sheared zone at many places (Figure 5.4g).There are two cases of the offsetting veins where majority shows dextral displacement (Figure 5.4g) while sinistral movement observed in one case. These are clear and strong evidence of the presence of fault crossing the river channel.

The fault from the north extends towards its SW and exposed to the east of Pipalava village. The fault passes over the jointed trappean lava flows of Deccan trap formation (Figure 5.5a). The prominent feature observed near fault zone is the presence of dyke that might have intruded along the fault line. The extension of the dyke is towards SW forming a ridge along the trend of the fault (Figure 5.5a). The trappean basalt observed is hard, compact with vertical to sub-vertical joints that are filled with recrystallized quartz and calcite veins (Figure 5.5b). A sharp lithological contrast of fractured basalt with zeolite minerals and compact basalt with striations is visible along the fault line (Figure 5.5b-d). Such similar dyke ridges and faults might be enclosed in nearby areas. The strike of the fault is ~N32º and vertical to sub-vertical fault plane shows very few faint striations. The sense of slip is inferred to be normal and with dip slip component (Figure 5.5d).

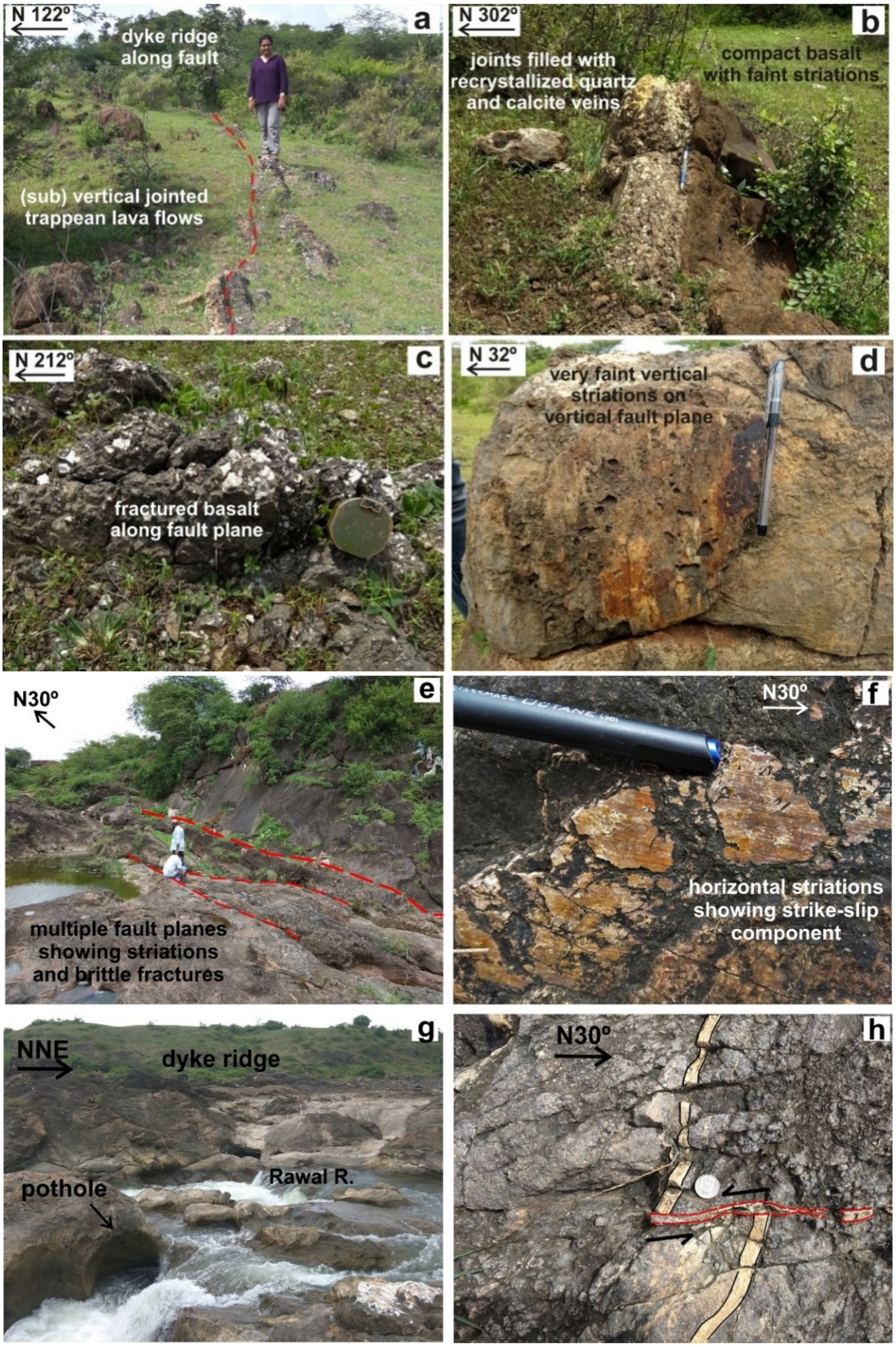

Figure 5.5 a) NE-SW trending fault (F2) near Pipalva village showing dyke intrusion along the fault in (sub) vertical joint planes in trappean lava flows. Note the extension of dyke ridge along the fault trend towards SW. b) (sub) vertical joint filled by recrystallized quartz and calcite veins along NE trending fault plane with fractured basalt (c) and compact basalt (d) on either sides. Very faint striations showing dip slip component. e) Fault (F2) near Mota Samdhiyala village showing multiple fault planes with brittle shear planes and striations. f) Faintly developed horizontal striations showing strike slip component. g) Fault passing the river showing brittle basaltic

rock, rapids and large potholes. Note the NNE-SSW trending dyke ridge. h) ~5 cm quartz vein offset on horizontal surface. Note the prominent bounding structure on displaced veins due to fractures along slip movement.

The extension of the fault (F2) towards SW swings NNE-SSW as evidenced by the multiple fault planes observed near Mota Samdhiyala village (Figure 5.5e). The strike of the fault is N30ºcrosses the south flowing Rawal River with the presence of all three types of striations. The horizontal striations observed are prominent (Figure 5.5f) compared to vertical and oblique striations. These striations are developed over vertical to sub vertical fault planes along with brittle shear zone with highly fractured basalt (Figure 5.5e-h). These slickensides inferred the sense of slip to be normal dextral, normal sinistral and strike-slip.The river flows over the fault zone incising the trappean bedrock forming several small rapids and large potholes (Figure 5.5g). The basalt shows prominent P- and Y- brittle shear planes over the fractured trappean channel bedrock. Numerous quartz and calcite veins filled in the basaltic rock is observed. These veins shows clear offset or displacement observed on the horizontal surface (Figure 5.5h). A quartz vein was observed showing 4.5 cm offset on the horizontal surface (Figure 5.5h). This displaced vein shows several boudin structures formed due to fractures along the slip movement (Figure 5.5h). This infers that shear zone is due to severe deformation forming transverse nature of the fault. However, few faintly developed vertical and oblique striations also explains that the fault might have undergone multiple reactivation.

The exposed fault (F2) from Khambha (north) to Mota Samdhaliya village (south) was detected, investigated and mapped to understand the topographical and geomorphic variation in study area. The Malan River flows along the fault trend towards coast. The fault is inferred to be buried under the pediment surface up to the coast. The evidences like striations on vertical to sub vertical fault plane, brittle shear zones, vein displacement, slicken fabrics etc. observed are prominent in all the locations on the exposed fault planes. These evidences strongly infers that it is an extensive fault which terminates the NE trending dyke swarms that swings coastward trending ~NNE-SSW.

5.1.3 Fault (F3)

From Timbi to Mota Mansa, a NE-SW trending basaltic ridge (~50m elevation) runs parallel to the main road was explored and observed till Mota Mansa (Figure 5.6a-d). The surrounding dyke ridges runs parallel to the fault between Raidi and Malan River basin. The exposed fault plane is observed at two locations: one at south of the Mota Mansa and other is at Mota Mansa village. The ridge shows multiple fault planes same as Katar Fault (F1) with prominent oblique and vertical striations (Figure 5.6a-c). The fault is showing normal sinistral slip by observing the smoothness and roughness criteria on the vertical fault plane. However, several attitudes of the fault plane is measured for fault-slip analyses. This fault ridge extends near Mota Mansa, where NE trending ridge is ~100 m elevation and fault plane is observed on the top of the ridge with prominent oblique as well as vertical striations. However, few horizontal striations were seen with very faintly developed striations (Figure 5.6d). Several other oblique to vertical striations were observed on the vertical fault planes exposed on the adjacent ridges (Figure 5.6e, f). These dyke ridges are part of the dyke swarms swinging coastward (towards south) trending NE. The fault-slip data of NE trending fault were collected for paleostress analyses.

5.1.4 Fault (F4)

Near Shana Vankiya, some ridges shows three types of prominent striation viz., horizontal and vertical (Figure 5.6g-h) on sub horizontal fault plane surface. The same ridge shows striation variations on opposite sides of road. Pure dextral strike slip fault with striations observed on two planes and the missing block moved eastward (Figure 5.6g-h). This was observed in field by roughness and smoothness criteria on fault plane. This shows highly fragmented terrain with structural complexity showing prominent fault evidences. Several other parallel dykes and/or ridges observed in the satellite images that needs to explore and investigate further to understand the fault dynamics around dyke swarm region.

Several other faults observed NE of Rajula town, east of Dhantarvadi River through remote sensing studies. However, these faults were observed by the satellite imageries showing NNW-SSE trending fault offsets several NE trending dyke ridges. These dyke swarms trend ENE towards eastern side of the study area further up to Palitana and Bhavnagar. The set of parallel NE-SW faults observed towards northeast of Rajula shows left lateral slip sense. All these faults have strong geomorphic expression in the form of NW facing scarp faces of the cuesta ridges. The tectonic movements along all the faults observed in morphotectonic domain-I shows varying fault plane attitudes. All these faults were exposed on the dyke ridges and extend along the trend of the dyke. This is a debatable issue that dykes might have intruded the faults after change in stress regime during Indian plate collision. However, the fault-slip data collected from all the faults observed to understand the stress pattern during the Cretaceous period.

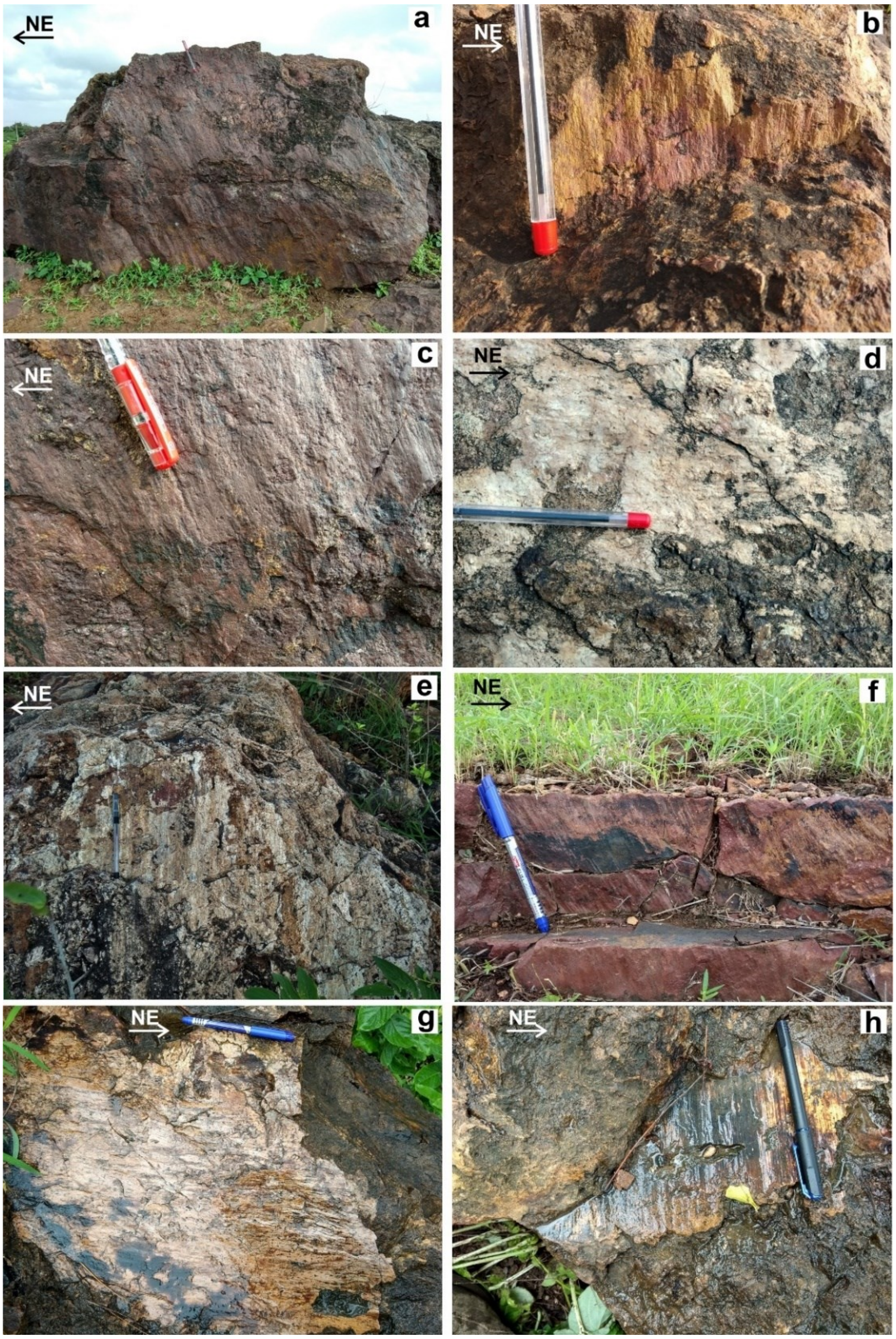

Figure 5.6 Faults exposed on the NE-SW trending ridges between Malan and Raidi river basin. 14.3 cm long pen as scale. a) Vertical undulating fault plane (attitude: 265° strike, 74° dip, 355° dip direction) with oblique striations. b) Fault plane (attitude: 270° strike, 80° dip, 355° dip direction) with vertical striations. c) Sub vertical fault plane (attitude: 262° strike, 77° dip, 353° dip direction) with oblique striations. d) Vertical fault plane (attitude: 275° strike, 60° dip direction) with horizontal direction. Fault near Mota Mansa village showing e) Faintly developed striations on vertical fault plane (attitude: 80° strike, 83° dip, 350° dip direction) and f) Prominent oblique striations on vertical fault plane (attitude: 55° strike, 65° dip, 140° dip direction).ENE trending fault showing sub horizontal fault plane (attitude: 80° strike, 23° dip, 345° dip direction) near Shana Vankiya with g) horizontal and h) vertical striations.

5.2 FAULT SLIP ANALYSES

Paleostress analysis is an important approach in order to define the orientation of principal stress axes in the study area. The fault-slip data includes fault plane orientation, sense of slip (normal/reverse/dextral/sinistral) and slickenside orientation. The data (attitudes of fault planes and slickensides) was used for fault slip analyses, using T-Tecto Studio X5, Win-Tensor (v5.8.7) and FaultKin (v7.7.2) (Appendix for working principles). These paleostress inversion software have been developed based on the assumption that the observed slip direction is parallel to the maximum resolved shear stress on the fault plane (Bott, 1959; Wallace, 1951). The data was collected from all the sites where faults are prominently exposed on the surface. There are in total four locations of prominent striations and fault slip data was collected, analyzed and mapped for the present study.

5.2.1 Katar Fault (F1)

A total of 46 fault-slip data of Katar Fault was used for fault slip analyses. The sense of movement along a fault plane is derived from one stress tensor that has been active during a certain period. Therefore, it is necessary to divide the heterogeneous fault-slip data into homogeneous subsets so as to determine paleostress state of the particular deformation event (Kounov, 2011). Homogeneous subset of data are those that are produced by a single deformation phase. The field photograph (Figure 5.3) shows cross-cutting relationship of two oblique slip striations and therefore it was difficult to determine the homogeneous subsets based on the striae superimposition criteria (Figure 5.7 a, b).

In such a scenario, separation of the heterogeneous fault-slip data was performed using T-Tecto software. The software separated the heterogeneous fault-slip data into homogeneous subsets of Phase 1 (Figure 5.7c) and Phase 2 (Figure 5.7d) by using the Gauss weighted right dihedra method (RDM). The Gauss method sort out the heterogeneous fault slip data into the homogeneous fault subsystems (Zalohar and Vrabec, 2007) and the RDM (Angelier, 1989 and references therein) calculates the stress tensor of each homogeneous fault subsystems. The results are shown in Figure 5.7 and Table 5.1. The phase 1 shows that maximum compressive stress (σ_1) is N315^o E and 94% of the fault set data represents this stress trend (Figure 5.7c). While phase 2 shows that the maximum compressive stress (σ_1) is N53^o E and 99% of the fault set data represents this trend (Figure 5.7d). Hence, the two deformation phases show entirely different trend of maximum principal horizontal stress. T-Tecto deduced stress ratio [$R= (\sigma_2-\sigma_3) \times (\sigma_1-\sigma_3)^{-1}$] ranging 0-0.2. The transpressive stress regime has prevailed as shown by the stress ratio (R) of 0 and 0.2 in Phase 1 and Phase 2 deformation event respectively generated by T-Tecto software. The advantage of paleostress analyses is that, R can be deduced which indicates the shape of the stress ellipsoid even though absolute stress magnitudes are not known (Fossen, 2016). For example R = 0, as obtained for “oblique-slip reverse fault with sinistral slip” faults (Figure 5.7, Table 5.1) indicates a prolate stress ellipsoid. Since, all the R values are << 1, none of the stress ellipsoids in these cases are oblate (uniaxial tension).

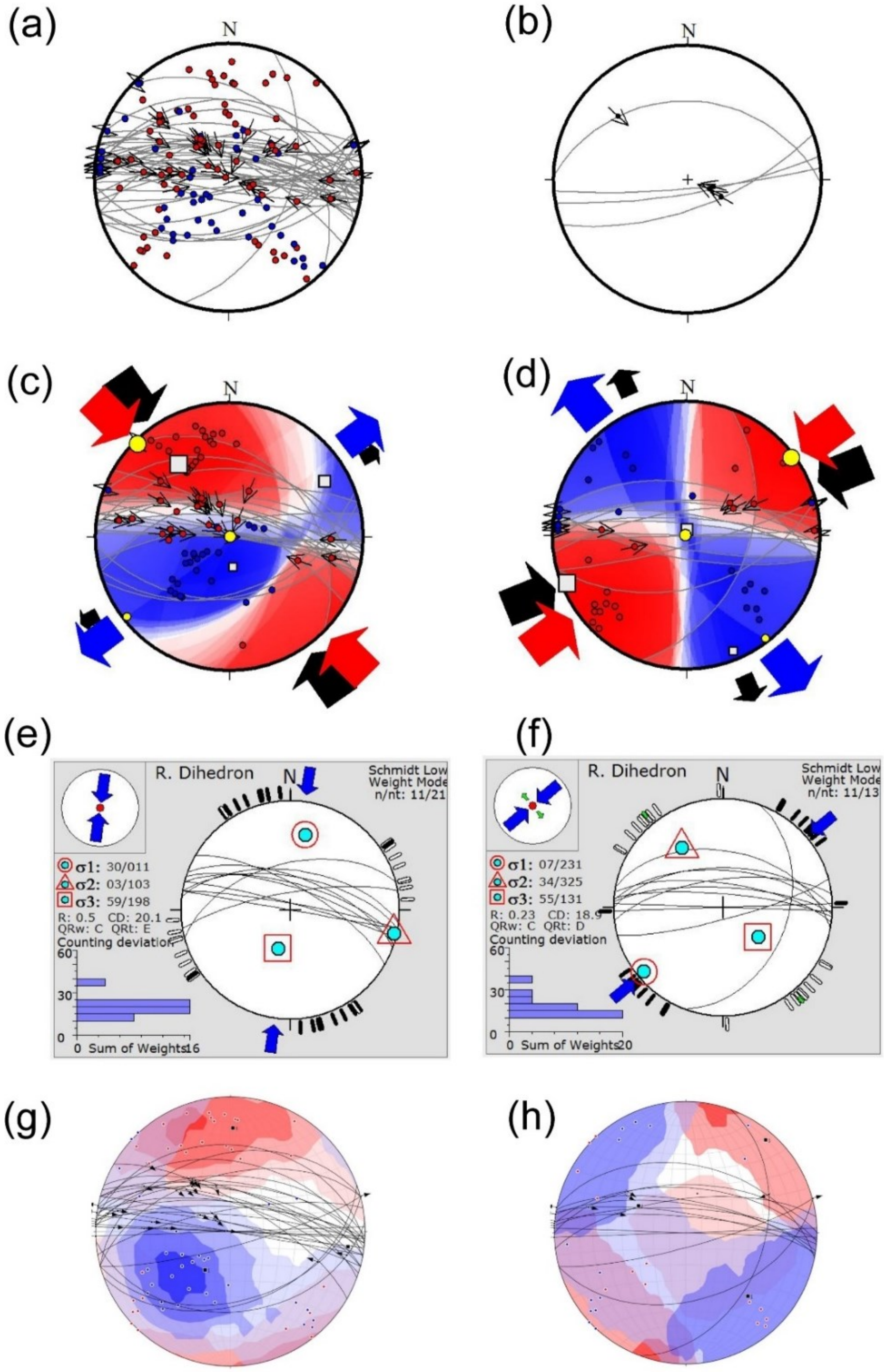

Figure 5.7 Results of fault-slip inversion analysis performed for heterogeneous fault-slip data using T-Tecto, WinTensor and FaultKin software (Vanik et al., 2018). (a)

Stereo plot (lower hemisphere) - grey lines: fault planes with slip vectors marked by black dot with arrows. Red and blue dots: direction of P- (compressive) and T (extension) kinematic axes for the individual fault plane respectively. (b) Stereo plot of fault planes misfit in the resultant tensor. (c) & (d) Resultant stress tensors of Phase 1 and Phase 2 deformation, respectively, generated from T-Tecto software. Squares: directions of principal stress axes obtained by the Gauss weighted Right Dihedra Method. Yellow circles: directions of principal strain axes by Visualization of Gauss Function method. Biggest square and yellow circle: direction of σ1; Medium square and yellow circle: direction of σ2; smallest square and yellow circle: direction of σ3. Red inward- and blue outward arrows: direction of compressive- and tensile stress, respectively. Red and blue quadrants of the graph: compressive and extensive strain fields, respectively. (e) & (f) show resultant stress tensor of Phase 1 and Phase 2 deformation generated from fault-slip inversion analysis for homogeneous subset of fault-slip data using WinTensor. Black lines: fault planes with slip vectors marked by open circles with arrows. Black solid lines and open lines at the periphery of the stereo-plots: direction of SHmax and SHmin kinematic axes, respectively, for individual fault slip data. Stress symbol in the upper left corner. The orientation of the principal axes of the stress ellipsoid and the stress ratio (R) suggest the stress regime. The length and color of the horizontal stress axes (SHmax and SHmin) in the stress symbol: horizontal deviatoric stress magnitude (Delvaux, 1997). The vertical stress (σv) is indicated by a blue (σ1) / green (σ2) / red (σ3) solid circle in the middle of the stress symbol suggesting the extensive/ strike-slip/ compressive stress regime. Stress tensors in the middle: blue inward arrows- compressional deviatoric stress (SHmax = σ1); red outward arrows: tensile deviatoric stress. Circle, triangle and square: direction of maximum principal stress (σ1), intermediate principal stress (σ2) and minimum principal stress (σ3), respectively. "n/nt": ratio of fault slip data used relative to the total number of fault slip data entered (Delvaux, 2003). The graph of counting deviation is shown at the lower left corner of the graph. (g) and (h) show fault-slip inversion analysis performed for homogeneous subset of fault-slip data using FaultKin. Stereo plots of resultant stress tensors of Phase 1 and Phase 2 deformation are shown respectively. Black lines- fault planes with slip vectors marked by a black dot with arrows. Red and blue dots: directions of P (compressive) kinematic axis and T (extension) kinematic axis for the individual faults, respectively. Red and blue contours: compressive and tensile strain fields, respectively. Green squares: the direction of the principal stresses.

Figure 5.7 and Table 5.1 avoided purely dip-slip normal- and reverse faults in the analyses. The separated homogeneous subsets of heterogeneous fault-slip data were then entered into WinTensor (Figure 5.7e, f) and FaultKin (Figure 5.7g, h) software. These were done in order to compare results obtained from T-Tecto, Win-Tensor and FaultKin. Win-Tensor software aided to deduce the stress axes attitudes for fault types (Figure 5.7e, f, Table 5.1) that can be compared with T-Tecto deductions (Figure 5.7c, d, Table 5.1). For oblique-slip reverse fault with sinistral slip, attitude of the σ_1-axis is 315° (trend) and 0° (plunge) as per T-Tecto (Figure 5.7c,

Table 4.1), and 11° (trend) and 30° (plunge) as per Win-Tensor (Figure 5.7e, Table 5.1).

Table 5.1 Fault slip analysis performed with T-Tecto studio X5, Win-Tensor and FaultKin for heterogeneous fault-slip data (as in Delvaux and Sperner, 2003; Allmendinger et al., 2012). The results are given as homogeneous subsets divided in Phase 1 and Phase 2 deformation. n: number of fault-slip data used in the inversion. σ1, σ2 and σ3: principal stress axes. Stress ratio R = (σ2 − σ3) × (σ1 − σ3) −1. Meaning of "Magnitude": for example for the underlined magnitude, 94% out of 23 fault data can be represented by 315° trend and 0° plunge (Vanik et al., 2018).

Sl. no.	Software	n	Fault type	σ_1			σ_2			σ_3			Stress ratio R (unit less)	***Stress regime*** *as per Delvaux (1997)*
				Trend **(in** degrees)	Plunge **(in** degrees)	Magnitude	Trend (in degrees)	Plunge (in degrees)	Magnitude	Trend (in degrees)	Plunge (in degrees)	Magnitude		
Phase 1														
1	T-Tecto	23	Oblique slip reverse, sinistral slip	315	0	<u>94%</u>	82	89	N/A	232	0	82%	0.2	**Transpressive**
2	WinTensor	11	Oblique slip reverse, sinistral slip	11	30	-	103	3	N/A	198	59	-	0.5	**Pure compressive**
3	FaultKin	23	Oblique slip reverse, sinistral slip	220.5	51.7	-	78.2	32	N/A	336	18.7	-	-	-
Phase 2														
4	T-Tecto	14	Oblique slip reverse, sinistral slip	53	0	99%	292	90	N/A	142	0	96%	0	**Transpressive**
5	WinTensor	11	Oblique slip reverse, sinistral slip	231	7	-	325	34	N/A	131	55	-	0.23	**Transpressive**

Comparing fault-slip analyses results summarized in Table 5.1, one notes a wide mismatch of attitudes of stress axes for different fault types, such as sl 1, 2 and 3. As per Anderson's theory, two of the stress axes remain horizontal and the third one vertical. This constrain is more closely obeyed by the T-Tecto results (Figure 5.7c, d, Table 5.1) than that by Win-Tensor (Figure 5.7e, f, Table 5.1). Incompatible fault-slip data has not been considered in the resultant stress tensor. The compatibility of the data is determined through the right dihedral method (e.g., Betka et al., 2016). One limitation of FaultKin software is that it cannot provide the R value. Subsequently, it is not possible in this method to visualize the shape of the stress ellipsoid.

5.2.2 Fault (F2)

A total of 25 fault-slip data of the NE to NNE trending fault (F2) were used for paleostress analyses using WinTensor software. The fault plane shows mostly oblique dip slip movement derived from the stress tensors. The attitude of the fault plane and the slickensides determine that it is normal dextral fault. The dip slip movement along the fault line is may be due to the extensional stress regime before the collision of Indian plate. However, the oblique slip and strike slip movement noticed in few fault-slip data defines the dextral movement of fault blocks due to right lateral slip. The stress tensors obtained from these data shows the NE-SW compression. The consistent fault-slip data generated the tensors of all the locations of the exposed fault plane. Unlike the Katar Fault, the separation of the data from heterogeneity was not required. The results of the fault-slip data (Figure 5.8a-c) shows the stress tensors calculated from different locations.

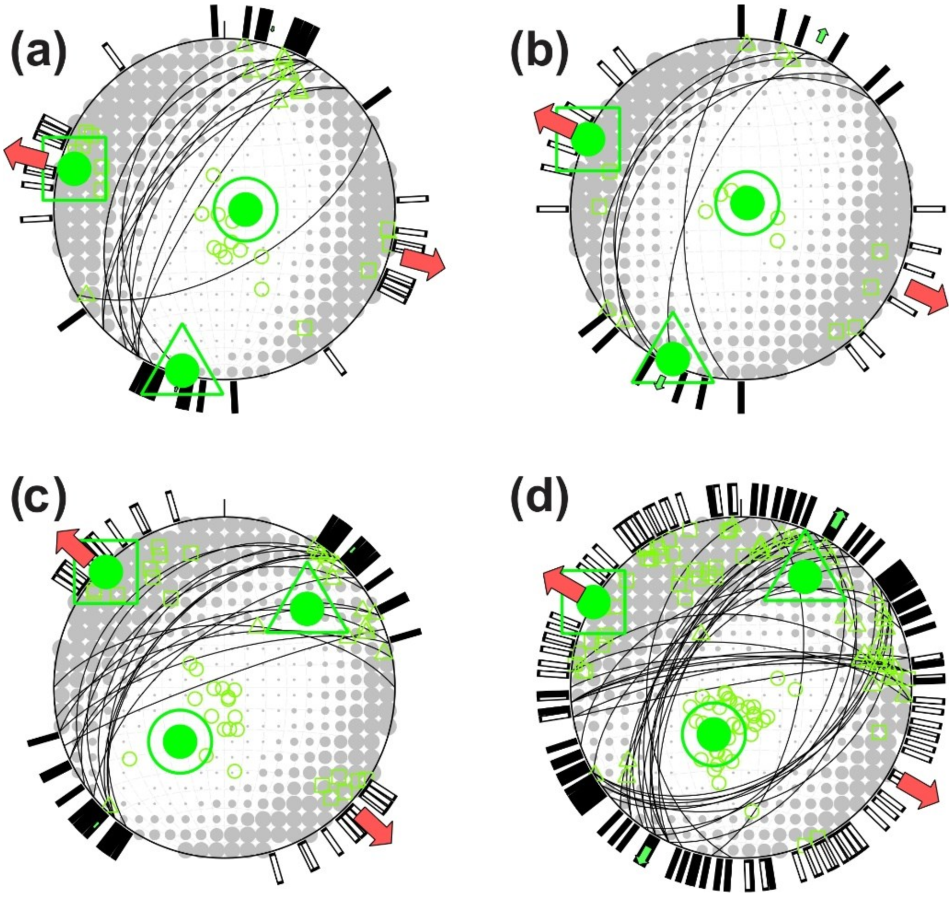

Figure 5.8 Resultant stress tensors obtained from fault-slip data using WinTensor software. Black lines: fault planes with slip vectors marked by open circles with arrows. Black solid lines and open lines at the periphery of the stereo-plots: direction of SHmax and SHmin kinematic axes, respectively, for individual fault slip data. Stress tensors: green inward arrow – compressional deviatoric stress (SHmax = σ1); red outward arrows – tensile deviatoric stress. Circle, triangle and square: direction of maximum principal stress (σ1), intermediate principal stress (σ2) and minimum principal stress (σ3), respectively. (a), (b) & (c) show resultant stress tensor from fault-slip data collected from exposed fault plane of Fault (2). (d) show resultant stress tensor from Fault (F3) near Mota Mansa village.

The fault-slip data at the north of the fault line shows that the maximum compressive stress (σ_1) is N20º E and maximum fault set data signifies this stress direction (Figure 5.8a). Further south, the maximum compressive stress (σ_1) is N26º E and N42º E and most of the data represents this stress trend (Figure 5.8b, c). This indicates that the area has experienced the deformation event during extensional stress regime because of pure dip slip movement. However, the oblique striations infers the reactivation of the fault after Indian plate collision. This occurred during the change in stress regime from extension to compression resulting into multiple striations. The fault is oblique slip normal fault with dextral slip and this fault is responsible for the termination of NE trending dyke swarms.

5.2.3 Faults (F3 and F4)

A total of 44 fault-slip data collected from the NE trending fault near Mota Mansa village for paleostress analyses using WinTensor software. The multiple fault planes with multiple striations observed in this fault comparable to Katar Fault. However, majority of the slickensides shows significant oblique slip movement. The fault is showing normal fault with sinistral slip. However, the sense of slip was observed in the field by roughness and smoothness criteria. The strike slip and dip slip component both signifies the extensional faults and its reactivation during compression. The stress tensors obtained from the fault-slip data shows these results (Figure 5.8d). The fault-slip data shows that the maximum compressive stress (σ_1) is N30^o E and majority of the data represents this stress direction (Figure 5.8d). The SHmax direction is NE-SW which also relates with the stress scenario of the other faults. The NE compression resulted in the reactivation of all the faults after the Indian-Eurasian plate collision period.

The faults observed in the trappean rocks observed with multiple fault planes and multiple striations exposed mainly in the dyke ridges showing prominent structural trend. These faults were activated when the terrain was experiencing extensional stress around 55 Ma back. All these faults got reactivated after the collision when the terrain was undergoing NE compression with the Indian plate movement. The stress tensors determines that a dip slip component in every fault plane mapped. However, the strike slip component also observed deduce the reactivation of the faults with minor change in stress trends. The maximum compressive stress ranges from N20^o E to N50^o E for the faults observed over the Deccan traps in the domain-I.

5.3 PALEOSTRESS ANALYSES (TERTIARY AND QUATERNARY JOINT SETS)

The pediment surface in domain-I is mostly covered by fossiliferous limestone of Gaj Formation with prominent two sets of joints sloping gently towards coast. The best exposures of Tertiary joints are located along the inferred E-W trending Katar fault near Pipavav, south of Kadiyali village (Figure 5.9). The Pipavav port is located ~10 km to the south of the study area near the vast intertidal flats. The abruptly terminating mudflats are observed towards east of this region along the fault trend. Small mound of the yellowish colored fossiliferous limestones observed shows prominent joint sets (Figure 5.9). The joint planes are almost vertical with a gently dip towards coast (Figure 5.9a). The Tertiary rocks also consisting of greyish colored compact limestone on the top underlain by yellowish fossiliferous limestone (Figure 5.9b). The greyish colored laminated calcareous shale lies beneath these rocks. The area is covered by compact fossiliferous limestone with two to three sets of joints on a (sub) horizontal surface. These joint patterns are also observed in the river sections where the joints data was collected for the analyses. The prominent joint sets observed are mostly conjugate joints (Figure 5.9d, e). There are irregular spacing in the open conjugate joints (Figure 5.9c-e). Few are 90^{o} to each other also called orthogonal joint sets observed on the (sub) horizontal surface (Figure 5.9f).

A total of 104 joint plane measurements are used in the analysis. The joints reported are dominantly of planar geometry and the spacing of the joint sets varies. The conjugate shear joints developed on the fossiliferous limestone showing oblique joints, dip joints and irregular joint spacing. Majority of the joint plane data were represented by vertical to sub-vertical dip (> 80°) with few joint planes dipping in 40˚ to 80˚ range. Joints with varying trend are documented. The joint sets are mainly NNE-SSW, NE-SW, NNW-SSE and NW-SE trending. The NNE-SSW and NE-SW trending joint planes are manually grouped together for paleostress determination and paleostress tensor is generated for the same. Joint planes trending NNW-SSE and NW-SE directions are also treated similarly.

The conjugate joint planes are also good paleostress indicators in order to reveal the tectonic stress field (Dyer, 1988; Mastella et al., 1997). Paleostress analysis results shows the resultant paleostress tensor obtained for joint planes trending in NNE-SSW and NE-SW directions. The stress tensors generated for two different joint planes. Total of 104 joint plane measurements are used in the analysis using T-Tecto X5 software. The program utilizes the Visualization of the Gauss object Function (VGF) method (Zalohar and Vrabec, 2007). This function performs the Gauss weighted Right Dihedra Method (RDM) in order to calculate the most probable orientation of maximum and minimum principal stress axes. A total of 65 joint sets measurements were used for NNE and NE trending joint planes. The paleostress tensor shows maximum compressive stress (σ1) as N46º E, intermediate principal stress (σ2) to be vertical, oriented in N267º E direction and the minimum compressive stress (σ3) is oriented N133º E (Figure 5.10a). Thus, the result shows ~NE-SW compression for joint planes trending NNE-SSW and NE-SW directions. Figure 5.10 shows the result of joint planes trending in NW-SE and NNW-SSE directions.

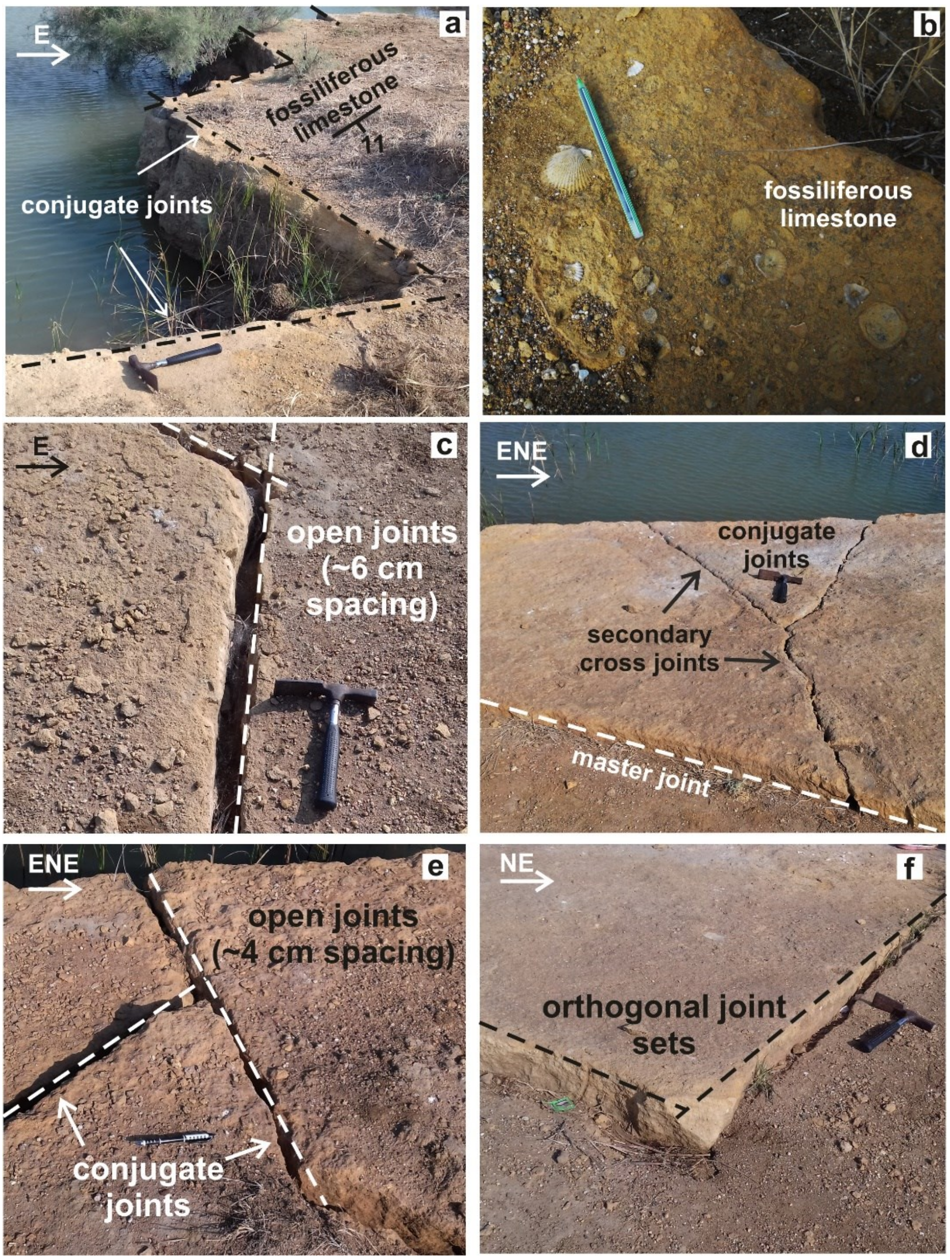

Figure 5.9 Tertiary joint sets data near Pipavav showing different types of joints on gently coastward dipping fossiliferous limestone. Scale: Hammer (30 cm). a) Conjugate joint sets with dihedral angle- 42°. Tertiary fossiliferous limestone dipping southward (strike 85°, dip 11° and dip direction SSE). b) Close view of fossiliferous limestone. 13.2 cm long pen used as scale. c) Cross joint sets with open joints showing ~6cm displacement. d) Master joint with secondary cross joints and prominent conjugate joint sets. e) Open joint sets with ~4 cm displacement forming conjugate joint sets. f) Orthogonal joints showing perpendicular joint sets at few places.

A total of 39 joint plane measurements are used in this analysis for NW and NNW trending joint planes. The resultant paleostress tensor shows completely different orientations of principal stress axes as compared to the previous one. The maximum compressive stress (σ1) is horizontal trending N134° E, intermediate principal stress (σ2) is vertical trending N252° E and the minimum compressive stress (σ3) is horizontal trending N46° E (Figure 5.10b). Thus, the resultant paleostress tensor shows ~NW-SE compression for joint planes trending NW-SE and NNW-SSE directions. The joint data suggests that the area was undergoing compression which resulted in conjugate shear joints. The SHmax trend is towards NE and NW which is indicative of regional NE compression along with local compressive stress due to the fault zones or massive intrusion.

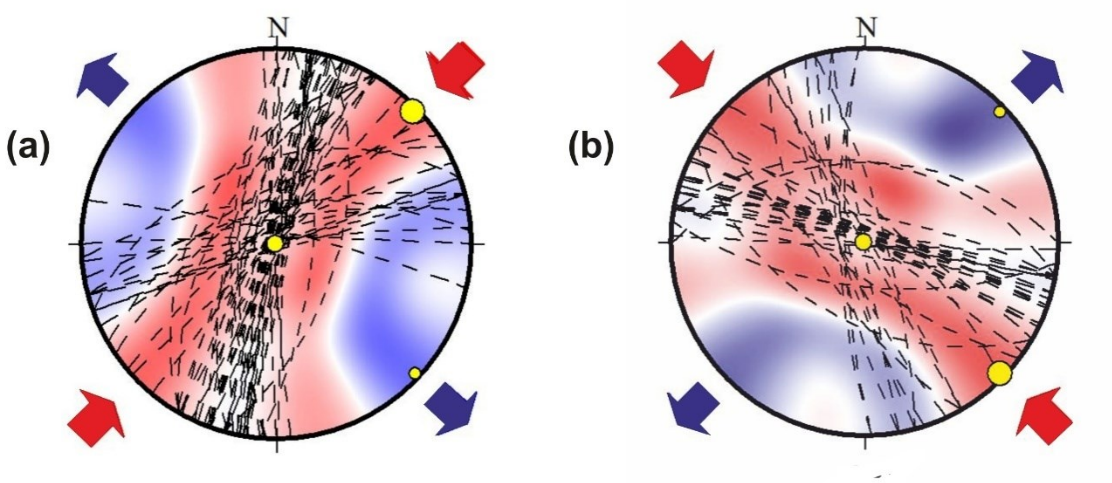

Figure 5.10 Resultant stress tensors generated from T-Tecto software of Tertiary joint sets. Yellow circles: directions of principal strain axes. Yellow circle- bigger circle: direction of σ1; Medium circle: direction of σ2; smallest circle: direction of σ3. Red inward- and blue outward arrows: direction of compressive- and tensile stress, respectively. Red and blue quadrants of the graph: compressive and extensive strain fields, respectively. a) NNE and NE trending joint planes showing SHmax N46°E. b) NW and NNW trending joint planes showing SHmax N134°E.

The Quaternary joint sets data largely observed in the morphotectonic domain-II were studied to understand the present maximum compressive stress trend. A total of 48 joint sets data were collected from the exposed river sections. Several joint planes on the miliolite beds observed on the horizontal surface. These joint planes show two prominent sets and formed knickpoints and small rapids. The joints might have appeared due to uplift and cooling effect later. The joints created blocks with less resistant rocks eroded due to retreating of river. These joints also show NNE compression in the SW Saurashtra. These area are comparable with the previously studied neotectonic joints in S and SE Saurashtra (Khadkikar, 2002; Bhonde and

Bhatt, 2009). The miliolitic joints sets data of the present study in domain-II is suggestive of post miliolitic compressive stress indicating that the area is still undergoing the NE compression.

5.4 INTERPRETATION OF STRESS PATTERN

The faults observed over the trappean lava flows and dyke ridges show the maximum compressive stress towards NE. The E-W trending Katar Fault determined the stress trend showing SHmax N53°E (Figure 5.11). However, faults observed along the NE-SW trending dyke swarms represent the SHmax from N20°E to N42°E. The stress scenario during the Deccan trap formation and the intruding dyke ridges deduce the anticlockwise stress rotation before the Indian plate collision. All these are extensional faults on brittle surface got reactivated when the subcontinent collided changing the stress regime to compressive. After the collision, during Miocene age, Tertiary rocks were deposited over the trappean lava flows. However, the NE compression was still undergoing that resulted into brittle shear joints on Tertiary rocks (Figure 5.11). Two prominent joint sets were observed and analysed resulting into two compressive trends. The SHmax trend N46°E and N134°E infer the regional stress and local perturbations. The Quaternary joint sets data towards east of the study area was studied by Bhatt and Bhonde (2009) showing NE-SW SHmax trend suggesting NE compression. The neotectonic joints in the SE Saurashtra was studied by Khadkikar, 2002 showing SHmax trend towards NE including other orientations i.e., NNE ENE and NW.

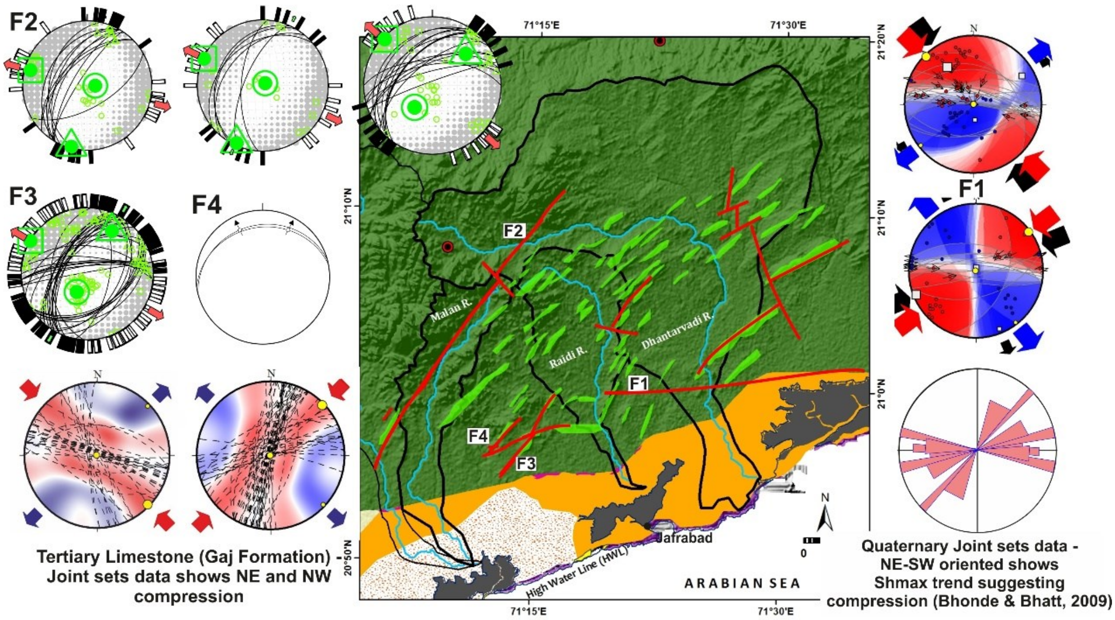

Figure 5.11 Resultant stress tensors from fault slip data and Tertiary joint sets data compared with Quaternary joints sets data of morphotectonic domain-I with field

photos. The rose diagram shows NE-SW major trend. Quaternary neotectonic joint set data showing NE-SW SHmax trend (Bhonde and Bhatt, 2009).

Gowd et al., (1992) determined N23° E trend of the horizontal maximum compressive stress (SHmax) by borehole breakouts, hydrofracturing and focal mechanisms from the Indian peninsula. SHmax results are also obtained by borehole data of Kundan et al., (2017) asN7° E in one well and as N40° E in another well drilled in Kachchh-Saurashtra basin (Kundan et al., 2017). Khadkikar (2002) also reported NE trending SHmax from studies on neotectonic joints at SE Saurashtra. Bhonde and Bhatt (2009) confirm the mean NE trend of SHmax from the coastline of S Saurashtra. The major stress trends plotted in the offshore region (I) σ1: N7° E and (II) σ1: N40° E differs from the stress tensors of the Katar Fault i.e., σ1: N53° E. The difference in orientation between maximum horizontal stresses (σ1) of fault (F1) to that to offshore region is (I) N46° E and (II) N13° E. This indicates that from the offshore region into the south Saurashtra, SHmax (corresponds to σ1) underwent a rotation.

The multiple SHmax trend in the faults are due to its reactivation during post-Deccan trap. The faults might have reactivated during Tertiary period along with the formation of joint sets. The stress rotation from the Early Cretaceous to Tertiary period shows that area underwent 7° anticlockwise rotation. These stress rotations are still active as the area has underwent 1° anticlockwise rotation from Tertiary to Quaternary period. The maximum compressive stress relations of faults over trappean rocks, Tertiary joint sets data and previously studied Quaternary joints in the present study area shows that the area has underwent 8° anticlockwise rotation.

Overall, the morphotectonic domain-I shows variably oriented striations on fault planes indicating multiple reactivation phases observed in all the mapped faults on Deccan Traps. These faults were used for paleostress analyses inferring compressional and extensional stress regime on the terrain. The rocks of Tertiary and Quaternary deposits shows prominent two to three sets of joints are mapped that have developed under compressional stress regime. In general, the morphotectonic domain-I shows evidences of reactivated faults, neotectonic joint sets, stream deflections, sharp channel bend, large potholes and knickpoints suggests the domain has been neotectonically active.